STUDIA UNIVERSITATIS BABEŞ-BOLYAI, CHEMIA, LV, 1, 2010

INVESTIGATION OF AZ91 MAGNESIUM ALLOY OXIDATION KINETICS BY MEANS OF ELECTROCHEMICAL IMPEDANCE SPECTROSCOPY

VALENTINA TASOTI[a], ADRIAN NICOARĂ[b,*] AND PAUL ŞERBAN AGACHI[a]

ABSTRACT. A magnesium alloy oxidation in alkaline solutions was investigated by electrochemical impedance spectroscopy. Recorded impedance spectra exhibited up to two capacitive loops, suggesting oxidation trough adsorbed intermediates. For a kinetic description of reaction mechanism, equation of the parameters of Voight-type electrical equivalent model were obtained and used for magnesium alloy oxidation in open circuit conditions.

Keywords: *Microarc oxidation, magnesium alloy, electrochemical impedance spectroscopy, kinetic mechanism*

INTRODUCTION

Magnesium alloys – which are increasingly used in automotive, aerospace and electronic industries – suffer for poor friction-reducing, anti-wear and corrosion resistance. Fortunately, these disadvantages can be significantly reduced by appropriate surface treatment techniques. Microarc oxidation is such a technique, which can be used to fabricate ceramic coatings on a various range of chemical active metals and their alloys [1-3]. As compared with other surface treatment techniques, microarc oxidation is economic efficient, easy to control, ecological friendly and versatile [4].

Microarc oxidation is an electrode process that combines conventional electrochemical oxidation with spark discharges, allowing the obtaining of a ceramic coating with good protective properties. It requires the use of high enough voltage to allow dielectric breakdown of formed oxide film, which occurs at discrete locations accompanied by spark discharges. These high-temperature and high-pressure discharges ensure not only the conditions indispensable for spinel formation from oxides, but also increase the oxidation rate [5].

[a] *Babes-Bolyai University, Department of Chemical Engineering and Material Science, 11 Arany Janos, 400028 Cluj Napoca, Romania*

[b] *Babes-Bolyai University, Department of Physical Chemistry, 11 Arany Janos, 400028 Cluj Napoca, Romania, anicoara@chem.ubbcluj.ro*

For better understanding of overall process a mathematic model was developed, describing distributions of electrical potential, charge flux and temperature [6]. In order to extend its predictive capabilities, further developments should include kinetic information about elementary reaction steps. In present study oxidation kinetics of AZ91 magnesium alloy (containing 9% Al and 1% Zn) was investigated by means of electrochemical impedance spectroscopy, in two electrolytes solutions, further denoted as solution no. 1 and no. 2, which are usual for microarc oxidation.

RESULTS AND DISCUSSION

Electrochemical impedance spectroscopy was chosen for its unique ability of revealing the response of the elementary reaction steps, by exhibiting in isolation a series of phenomena. Each slow enough phenomenon will exhibit a loop with increasing diameter as its rate decreases, whereas the time-constant is increasing as the inertia of corresponding phenomenon increases. Examples of such phenomena with corresponding time-constant (usually) increasing in mentioned order are: charge conduction by migration, charge balance, mass transport, surface relaxation with adsorbed intermediates and electrocrystallization. Only migration has negligible inertia, thus its elementary response, namely the ohmic resistance (R_Ω), is frequency-independent.

The plots of measured electrochemical impedance are presented in Fig. 1, exhibiting a high-frequency capacitive loop, with an additional low-frequency capacitive loop only in the case of solution no. 2. The high-frequency loop was assigned to charge balance phenomenon; its characteristics are the loop diameter, defined as charge transfer resistance (R_{ct}), and time-constant ($\tau_c = R_{ct}C_d$) which is also influenced by the double-layer capacity (C_d). The low-frequency loop was assigned to a phenomenon of surface relaxation with adsorbed intermediates and has as characteristics the adsorption resistance (R_a), defined as diameter of loop, and adsorption time-constant (τ_a). The absence of some other low-frequency loops, assignable to mass transport and electrocrystallization phenomena, proves that these elementary steps are fast enough to be ignored when modelling the process.

Qualitatively, charge transfer is the slowest elementary step and is marginally influenced by electrolyte concentration. Conversely, the surface relaxation loop is much more influenced by electrolyte concentration, whereas the contribution of this phenomenon to overall process is minor.

To quantify these phenomena, the experimental impedance spectra are fitted with a *Voight*-type electrical equivalent model, constructed by serial connection between the ohmic resistor and two parallel resistor-capacitor elements [7]. The fitting model describing the influence of frequency on impedance's modulus is:

$$|Z(f)| = \left\{ \left[R_\Omega + \frac{R_{ct}\left(1 + 2\pi f R_{ct} C_d \sin\alpha\right)}{1 + 4\pi f R_{ct} C_d \sin\alpha + (2\pi f R_{ct} C_d)^2} + \frac{R_a}{1 + (2\pi f \tau_a)^2} \right]^2 + \right.$$

$$\left. + \left[\frac{2\pi f R_{ct}^2 C_d \cos\alpha}{1 + 4\pi f R_{ct} C_d \sin\alpha + (2\pi f R_{ct} C_d)^2} + \frac{2\pi f R_a \tau_a}{1 + (2\pi f \tau_a)^2} \right]^2 \right\}^{1/2} \quad (1)$$

and is employed for calculation of the following model parameters: R_Ω, R_{ct}, C_d, R_a, τ_a and α; the last one, without kinetic relevance, describes the flattening of loop caused by electrode roughness [8].

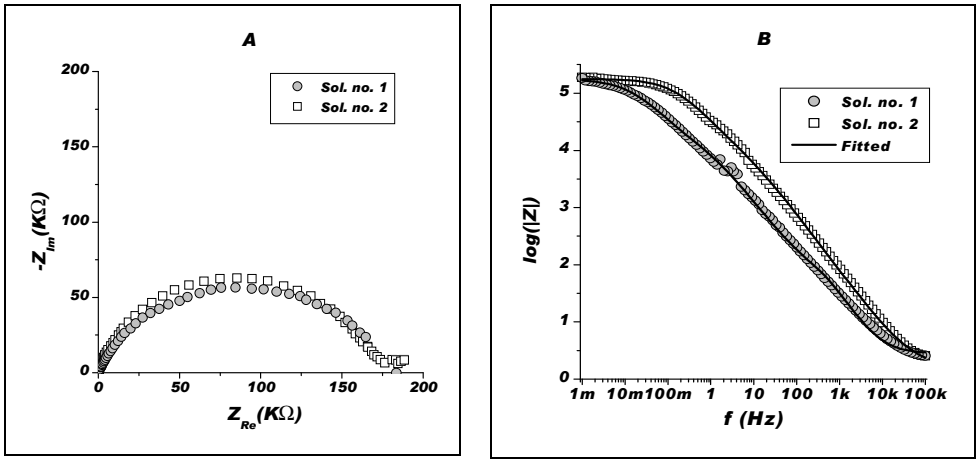

Figure 1. Measured spectra as complex-plane (A) and Bode (B) impedance plots, for oxidation of A791 alloy in electrolyte solutions presented in legend. In addition, in (B) fitted spectra are also presented as solid lines

The fittings were performed utilizing the nonlinear Levemberg-Marquardt algorithm implemented on Microcal Origin® 6.1. The results of this iterative fitting procedure are presented in Table 1 (line A) as estimates of the value and of the standard error, for 0.95 level of confidence, of the above-mentioned model parameters. Being kinetic relevant, the average of measured dc current is also presented in Table 1.

Although useful in describing the behaviour of elementary phenomena, Voight model parameters can be further correlated with the rates of elementary reaction through a herein developed mathematic model. In order to maintain the model complexity into reasonable limits, only the behaviour of magnesium, the main constituent of the AZ91 alloy, was taken into account.

Table 1. Results of fitting procedures: A) electrical equivalent circuit parameters obtained by fitting experimental spectra; B) fitting of the obtained parameters leading to the kinetic parameters (rate constants and symmetry factors) presented in text.

Fitted data/ Fitting model	Sol.	I (nA)	R_{ct} (kΩ)	R_a (kΩ)	τ_a (s)	R_Ω (Ω)	C_d (μF)	α (rad)
A. Experimental spectra/ Eq. (1)	1	4.9±1.6[(a)]	174±9	–[(b)]	–[(b)]	2.1±0.4	9.3±0.9	0.72±1.0
	2	4.2±1.8[(a)]	169±14	20±8	61±19	1.6±0.2	2.5±0.3	0.76±1.2
B. Electric parameters/ Eqs. (2); (11); (17); (26)	1	4.97	176	2.31	100.9	without kinetic relevance		
	2	4.32	169	19.9	60.7			

(a) the average measured of dc current; (b) data unavailable due to the absence of low-frequency loop.

The chemical mechanism is considered as follows:

$$Mg_{(s)} \underset{k_{-1}}{\overset{k_1}{\Leftrightarrow}} Mg^{+}_{(ads)} + e^{-} \quad \text{(R1)}$$

$$Mg^{+}_{(ads)} + 2OH^{-} \underset{k_{-2}}{\overset{k_2}{\Leftrightarrow}} Mg(OH)_{2(ads)} + e^{-} \quad \text{(R2)}$$

$$Mg(OH)_{2(ads)} \overset{k_3}{\Rightarrow} Mg(OH)_{2(s)} \quad \text{(R3)}$$

The faradaic current (I_F) and the coverage fractions of the adsorbed species generated by the two oxidation steps (θ_1, θ_2) are introduced by the charge (in steady-state) and the mass balance equations:

$$\frac{I_F}{AF} = k_1(1-\theta_1-\theta_2) - k_{-1}\theta_1 + k_2 C_{OH^-}\theta_1 - k_{-2}\theta_2 \quad (2)$$

$$\Gamma_{\max_1}\frac{d\theta_1}{dt} = k_1(1-\theta_1-\theta_2) + k_{-2}\theta_2 - k_{-1}\theta_1 - k_2 C_{OH^-}\theta_1 \quad (3)$$

$$\Gamma_{\max_2}\frac{d\theta_2}{dt} = k_2 C_{OH^-}\theta_1 - k_{-2}\theta_2 - k_3\theta_2 \quad (4)$$

where: A is the electrode area, F is the Faraday number, C_{OH^-} the interfacial concentration of OH^- and $\Gamma_{\max i}$ are the maximum surface concentrations of corresponding adsorbed species. In addition, k_1, k_2 and k_{-1}, k_{-2} are the rate constants of considered elementary reaction steps during oxidation and reduction, respectively; k_3 reflects the coverage clearing steps, like surface diffusion towards growing crystallites.

An important feature of the electrochemical impedance spectroscopy is the possibility of operating measurements in steady-state conditions.

Accordingly, steady-state coverage fractions can be easily calculated using the mass balance equations, by assuming solely their time-independence. The obtained equations are:

$$\theta_1 = \frac{1}{1+\frac{k_{-1}}{k_1}+\frac{k_2 C_{OH-}}{k_1}+\left(1-\frac{k_{-2}}{k_1}\right)\frac{k_2 C_{OH-}}{k_{-2}+k_3}} \tag{5}$$

$$\theta_2 = \frac{1}{1+\frac{k_3}{k_1}+\left(1+\frac{k_{-1}}{k_1}\right)\frac{k_{-2}+k_3}{k_2 C_{OH-}}} \tag{6}$$

The faradaic impedance (Z_F) can be obtained by taking into account the function of state nature of faradaic current, namely $I_F=I_F(E, \theta_1, \theta_2)$ as can be seen in eq. (2). In absence of experimental evidence supporting the contribution of mass transport to the overall process, C_{OH^-} was not considered as an associate variable. Consequently, faradaic current differential is the exact differential expression:

$$dI_F = \left.\frac{\partial I_F}{\partial E}\right|_{\theta_1,\theta_2} dE + \left.\frac{\partial I_F}{\partial \theta_1}\right|_{E,\theta_2} d\theta_1 + \left.\frac{\partial I_F}{\partial \theta_2}\right|_{E,\theta_1} d\theta_2 \tag{7}$$

and can be used to introduce the faradaic impedance as:

$$\frac{1}{Z_F} \equiv \frac{dI_F}{dE} = \left.\frac{\partial I_F}{\partial E}\right|_{\theta_1,\theta_2} + \left.\frac{\partial I_F}{\partial \theta_1}\right|_{E,\theta_2} \frac{d\theta_1}{dE} + \left.\frac{\partial I_F}{\partial \theta_2}\right|_{E,\theta_1} \frac{d\theta_2}{dE} \tag{8}$$

The three partial derivatives of faradaic current are calculated assuming common exponential activation of reaction rates for an electrochemical processes (i=1,2), namely:

$$k_i = k_i^o \exp\left[(1-\beta_i)\frac{F}{RT}(E-E_i^o)\right] \tag{9}$$

$$k_{-i} = k_{-i}^o \exp\left[-\beta_i \frac{F}{RT}(E-E_i^o)\right] \tag{10}$$

The newly introduced terms are as follows: k^o_i are standard rate constants, β_i the transfer coefficients, E_i^o the standard potentials and R is the gas constant. The obtained equations for the partial derivatives are:

$$\left.\frac{\partial I_F}{\partial E}\right|_{\theta_1,\theta_2} \equiv \frac{1}{R_{ct}} = \frac{F^2 A}{RT}\left[(1-\beta_1)k_1(1-\theta_1-\theta_2)+\beta_1 k_{-1}\theta_1+(1-\beta_2)k_2 C_{OH^-}\theta_1+\beta_2 k_{-2}\theta_2\right] \tag{11}$$

$$\left.\frac{\partial I_F}{\partial \theta_1}\right|_{E,\theta_2} = -FA(k_1 + k_{-1} - k_2 C_{OH-}) \tag{12}$$

$$\left.\frac{\partial I_F}{\partial \theta_2}\right|_{E,\theta_1} = -FA(k_1 + k_{-2}) \tag{13}$$

where eq. (11) introduces the charge transfer resistance (R_{ct}).

The calculation of the remanding terms from eq. (8) requests differentiation of the mass balance equations, after a prior transformation of time-dependent variables into frequency-dependent ones by means of Fourier transform. If M_1 denotes the right-hand side of eq. (3), one obtains:

$$j\omega\Gamma_{\max_1} d\theta_1 = \left[\left.\frac{\partial M_1}{\partial E}\right|_{\theta_1,\theta_2}\right] dE + \left[\left.\frac{\partial M_1}{\partial \theta_1}\right|_{E,\theta_2}\right] d\theta_1 + \left[\left.\frac{\partial M_1}{\partial \theta_2}\right|_{E,\theta_1}\right] d\theta_2 \tag{14}$$

where j is the complex operator and ω, the pulsation. Similarly, by denoting with M_2 the right-hand side of eq. (4), after a convenient rearrangement, the equations of coverage fractions total derivatives become:

$$\frac{d\theta_1}{dE} = \frac{A_{1,1}(1 + j\omega\tau_2) + A_{1,2}A_{2,1}}{(1 + j\omega\tau_1)(1 + j\omega\tau_2) - A_{1,2}A_{2,2}} \tag{15}$$

$$\frac{d\theta_2}{dE} = \frac{A_{2,1}(1 + j\omega\tau_1) + A_{1,1}A_{2,2}}{(1 + j\omega\tau_1)(1 + j\omega\tau_2) - A_{1,2}A_{2,2}} \tag{16}$$

where we defined the relaxation time-constants of adsorbed species (τ_i) and several *ad hoc* kinetic terms ($A_{i,j}$) as:

$$\tau_1 = -\Gamma_{\max_1} \Big/ \left.\frac{\partial M_1}{\partial \theta_1}\right|_{E,\theta_2} = \frac{\Gamma_{\max_1}}{k_1 + k_2 C_{OH-} + k_{-1}} \tag{17}$$

$$\tau_2 = -\Gamma_{\max_2} \Big/ \left.\frac{\partial M_2}{\partial \theta_2}\right|_{E,\theta_1} = \frac{\Gamma_{\max_2}}{k_{-2} + k_3} \tag{18}$$

$$A_{1,1} = -\left.\frac{\partial M_1}{\partial E}\right|_{\theta_1,\theta_2} \Big/ \left.\frac{\partial M_1}{\partial \theta_1}\right|_{E,\theta_2} = \frac{F}{RT}\frac{(1-\beta_1)k_1(1-\theta_1-\theta_2) + \beta_1 k_{-1}\theta_1 - (1-\beta_2)k_2 C_{OH-}\theta_1 - \beta_2 k_{-2}\theta_2}{k_1 + k_2 C_{OH-} + k_{-1}} \tag{19}$$

$$A_{1,2} = -\left.\frac{\partial M_1}{\partial \theta_2}\right|_{E,\theta_1} \Big/ \left.\frac{\partial M_1}{\partial \theta_1}\right|_{E,\theta_2} = \frac{k_{-2} - k_1}{k_1 + k_2 C_{OH-} + k_{-1}} \tag{20}$$

$$A_{2,1} = -\left.\frac{\partial M_2}{\partial E}\right|_{\theta_1,\theta_2} \Big/ \left.\frac{\partial M_2}{\partial \theta_2}\right|_{E,\theta_1} = \frac{F}{RT}\frac{(1-\beta_2)k_2 C_{OH-}\theta_1 + \beta_2 k_{-2}\theta_2}{k_{-2} + k_3} \tag{21}$$

$$A_{2,2} = -\left.\frac{\partial M_2}{\partial \theta_1}\right|_{E,\theta_2} \Big/ \left.\frac{\partial M_2}{\partial \theta_2}\right|_{E,\theta_1} = \frac{k_2 C_{OH^-}}{k_{-2} + k_3} \tag{22}$$

Finally, the equation of faradaic impedance becomes:

$$\frac{1}{Z_F} = \frac{1}{R_{ct}} - FA\frac{(k_1 + k_{-1} + k_2 C_{OH^-})[A_{1,1}(1 + j\omega\tau_2) + A_{1,2}A_{2,1}] + (k_1 + k_{-2})[A_{2,1}(1 + j\omega\tau_1) + A_{1,1}A_{2,2}]}{(1 + j\omega\tau_1)(1 + j\omega\tau_2) - A_{1,2}A_{2,2}} \tag{23}$$

This equation describes the faradaic impedance for the proposed reaction mechanism and exhibits a relaxation phenomenon (i.e., semicircular loop on complex plane representation) for each adsorbed intermediates. In investigated frequency range, maximum one adsorption-related relaxation phenomenon can be evidenced experimentally, allowing us to simplify eq. (23). For instance, if $\tau_2 << \tau_1$, one can approximate $1+j\omega\tau_2 \approx 1$; that is, the loop related to surface relaxation of the $Mg(OH)_{2(ads)}$ is exhibited only at frequencies lower than those used experimentally. This particular simplifying case was further considered because this loop emerges only for high C_{OH^-}. Thus, its corresponding time-constant must be function of C_{OH^-} and, because only eq. (17) fulfils this condition, it allows us to consider the assumption reasonable. In these conditions, the equation of faradaic impedance becomes:

$$\frac{1}{Z_F} = \frac{1}{R_{ct}} - FA\frac{(k_1 + k_{-1} + k_2 C_{OH^-})(A_{1,1} + A_{1,2}A_{2,1}) + (k_1 + k_{-2})[A_{2,1}(1 + j\omega\tau_1) + A_{1,1}A_{2,2}]}{1 - A_{1,2}A_{2,2} + j\omega\tau_1} \tag{24}$$

To calculate the adsorption resistance (R_a), one has to first calculate the faradaic impedance for infinite small frequency:

$$\left.\frac{1}{Z_F}\right|_{\omega\to 0} = \frac{1}{R_{ct}} - FA\frac{(k_1 + k_{-1} + k_2 C_{OH^-})(A_{1,1} + A_{1,2}A_{2,1}) + (k_1 + k_{-2})(A_{2,1} + A_{1,1}A_{2,2})}{1 - A_{1,2}A_{2,2}} \tag{25}$$

After using its definition, it leads to:

$$R_a \equiv Z_F\big|_{\omega\to 0} - R_{ct} = \frac{1}{\dfrac{1}{R_{ct}} - FA\dfrac{(k_1 + k_{-1} + k_2 C_{OH^-})(A_{1,1} + A_{1,2}A_{2,1}) + (k_1 + k_{-2})(A_{2,1} + A_{1,1}A_{2,2})}{1 - A_{1,2}A_{2,2}}} - R_{ct} \tag{26}$$

In conclusion, the impedance analytic model allows the formulation of a series of variables that contain kinetic information, namely I_F, R_{ct}, R_a and $\tau_a \equiv \tau_1$, all explicitly dependent on rate constants of the elementary reaction steps.

Calculation of the individual reactions rate constants was performed using another non-linear fitting procedure with the Levemberg-Marquardt algorithm. The dependent variable in this case is a vector with I_F, R_{ct}, R_a and τ_a as components, whereas C_{OH^-} is the independent variable and the model coefficients are the kinetic parameters (k_1, k_{-1}, k_2, k_{-2}, k_3 and β_1). In order to avoid solving an underdetermined mathematical problem, values for two other parameters were attributed (β_2=0.5, Γ_{max1} =1.62 10^{-9} mol cm^{-2}). The attributed value for transfer coefficient is common and should not influence significantly the obtained results if reaction (R2) is a fast one. Γ_{max1} was theoretically calculated under following assumptions: compact packing of magnesium atoms with 1.72 10^{-8} cm atomic radius.

The fitting results consist in model parameters estimates (k_1=1.65 10^{-12} mol cm^{-2} s^{-1}, k_{-1}= 10^{-14} mol cm^{-2} s^{-1}, k_2=8.8 10^{-9} cm s^{-1}, k_{-2}=8 10^{-12} mol cm^{-2} s^{-1}, k_3=10^{-11} mol cm^{-2} s^{-1} and β_1=0.39) and calculated dependent variables, presented in Tab. 1 line (B), which are in very good correlation with those obtained on impedance spectra fitting, presented in Tab. 1 line (A). To further compare the obtained values, one should use the values of apparent rate constant ($k_2' \equiv k_2 C_{OH^-}$), being 1.3 10^{-11} mol cm^{-2} s^{-1} and 2.6 10^{-11} mol cm^{-2} s^{-1} for solution no. 1 and 2, respectively.

The determined values suggest that the first oxidation step (R1) is relatively slow and thermodynamically irreversible, whereas the second oxidation step (R2) is significantly faster and rather reversible. The last considered step, that of coverage clearing (R3), is also a fast step and no further evidence about its reversibility can be obtained by the analysis of the presented data. More importantly, although oxidation takes place in a succession of reversible and irreversible steps, under given experimental conditions the slowest step is reaction (R1). However, the experimental evidencing of adsorption-related relaxation phenomenon makes imperative to take into account the reaction steps in which the adsorbed intermediate is involved, especially when a nonstationary model is considered.

Another important kinetic feature found is the difference between symmetry factors of the two oxidation elementary steps. In the investigated case, by increasing the potential, the reaction (R1) is favoured in comparison with reaction (R2), as it can be seen in eq. (9). Unlike in the present study, when the open circuit potential is applied, a much higher potential must be employed in order to sustain microarc oxidation, condition in which reaction (R2) could even be slower than (R1).

Further studies, especially aiming the influence of temperature, are requested for a realistic kinetic description of the microarc oxidation process. Because direct investigation of the microarc oxidation is rather difficult, mainly due to its intrinsic nonstationarity, the electrochemical impedance spectroscopy can provide both qualitative and quantitative information about the discussed process even if the investigation is performed in more convenient conditions.

EXPERIMENTAL SECTION

The working electrode made of AZ91 magnesium alloy was cut to 1cm^2. Prior to being use it was polished, with up to 2500 grid paper under ethanol, cleaned in an ultrasonic bath and then dried with cold air. A saturated calomel electrode and a platinum counter electrode, with surface of 2 cm^2, completed the employed conventional three-electrode setup. To improve the signal-to-noise ratio, the electrochemical cell was introduced into a Faraday cage.

The two employed electrolyte solutions were made up in distilled water, both containing 0.5M KF and 0.25M Na_3PO_4; in addition, 1.5 or 3M of KOH, and 0.5 or 1M of $NaAlO_2$ was employed when preparing solutions no. 1 or no. 2, respectively. Analytical grade reagents were used in all cases.

Electrochemical impedance spectroscopy measurements were undertaken using an Autolab PGSTAT 302 (Eco Chemie, The Nederlands) potentiostat equipped with FRA2 module. Impedance spectrums were obtained at open circuit potential (of -1.21 V *vs.* SCE), at 25±1 ^oC, using perturbation of 10 mV amplitude.

ACKNOLEDGEMENTS

One of the authors, V. Tasoti, gratefully acknowledges Dr. Patrik Schmutz (Swiss Federal Laboratories for Materials Testing and Research, Dübendorf, Switzerland) for providing the facilities for carrying out the experimental part of this work and for fruitful discussions.

REFERENCES

1 J. Liang, B. Guo, J. Tian, H. Liu, J. Zhou, T. Xu, *Applied Surface Science*, **2005**, *252*, 345.

2 P.I. Butyagin, Ye.V. Khokhryakov, A.I. Mamaev, *Materials Letters,* **2003**, *57*, 1749.

3 Y. Wang, T. Lei, B. Jiang, L. Guo *Applied Surface Science,* **2004**, *233*, 258.

4 S. Verdier, M. Boinet, S. Maximovitch, F. Dalard, *Corrosion Science,* **2005**, *47*, 1429.

5 Y.Q. Wang, K. Wu, M.Y. Zheng, *Surface Coating Technology*, **2006**, *201*, 353.

6 V. Tasoti, S. Agachi, J. P. Caire, *Proceedings of 30th International Conference of Slovak Society of Chemical Engineering*, **2003**, *1*, P146 1-6.

7 J. R. Macdonald, "Impedance spectroscopy Emphasizing solid materials and systems", John Wiley and Sons, New York, **1987**, p. 179-188.

8 F. Berthier, J.-P. Diard, R. Michel, *Journal of Electroanalytical Chemistry,* **2001**, *510*, 1.